

A Mouthguard-type Biosensor for Direct Measurement of Glucose Intake in Drinks

Kenta Ichikawa,^{1†} Kenta Iitani,^{1†} Yumin Zhao,²
Koji Toma,^{1,3} Takahiro Arakawa,^{1,4} and Kohji Mitsubayashi^{1,2*}

¹Department of Biomedical Devices and Instrumentation, Institute of Biomaterials and Bioengineering, Tokyo Medical and Dental University (TMDU), 2-3-10 Kanda-Surugadai, Chiyoda-ku, Tokyo 101-0062, Japan

²Graduate School of Medical and Dental Sciences, Tokyo Medical and Dental University (TMDU), 1-5-45 Yushima, Bunkyo-ku, Tokyo 113-8510, Japan

³Department of Electronic Engineering, College of Engineering, Shibaura Institute of Technology, 3-7-5 Toyosu, Koto-ku, Tokyo 135-8548, Japan

⁴Department of Electric and Electronic Engineering, Tokyo University of Technology, 1404-1 Katakura, Hachioji City, Tokyo 192-0982, Japan

(Received June 28, 2024; accepted January 16, 2025)

Keywords: cavitas sensors, saliva glucose, enzymatic biosensor, wearable sensor, Bluetooth Low Energy

Glucose in drinks is one of the key factors in the management and prevention of diabetes. Although several systems have been developed to monitor blood glucose levels as an indicator of diabetes, information on the actual intake of nutrients and their amounts is more effective for improving dietary habits. In this study, to evaluate the actual amount of glucose intake, we proposed a mouthguard-type sensor with an enzymatic biosensor for the direct measurement of the glucose concentration of ingested drinks. The fabricated biosensor was capable of quantifying glucose concentrations in the range of 1 μM –1 mM and showed measurement results equivalent to those of glucose measurement kits for some commercial drinks. The mouthguard-type sensor also showed quantification characteristics equivalent to the biosensor in wired measurements. In addition, wireless measurements with a mouthguard-type sensor were also demonstrated using a Bluetooth Low Energy potentiostat. These results suggest the potential application of real-time glucose intake measurement with the proposed mouthguard-type sensor.

1. Introduction

Type 2 diabetes is a worldwide lifestyle disease that can lead to severe complications such as diabetic retinopathy and diabetic nephropathy.⁽¹⁾ One of the causes of type 2 diabetes is the insufficient action of insulin due to unbalanced diets high in calories and fat.⁽²⁾ For the treatment, diagnosis, and prevention of diabetes, wearable sensors for the continuous measurement of blood glucose levels have been developed.^(3–5) Although blood glucose level is a medically important indicator that reflects the diet,⁽⁶⁾ having data on “what types and amounts of nutrients were consumed” could be more effective for improving dietary habits.⁽⁷⁾ Recently, systems for

*Corresponding author: e-mail: m.bdi@tmd.ac.jp

†These authors contributed equally to this work.

<https://doi.org/10.18494/SAM5210>

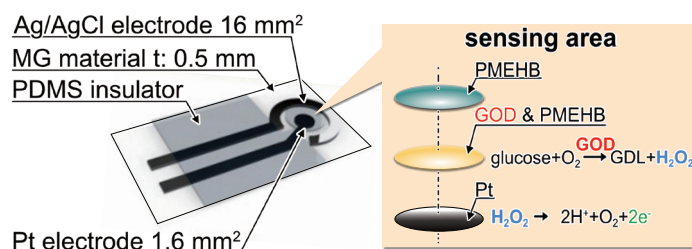
calculating the nutrients contained in a diet from photographs have been in practical use.^(8,9) However, the estimation of these systems is only based on the image information, and their accuracy and reliability are low. If the nutrients contained in the food and drink that are actually ingested can be directly measured, a more accurate monitoring of dietary habits can be achieved.^(10,11)

Intraoral sensors^(12,13) can directly access the food and drink ingested and can be implemented noninvasively, making them effective for monitoring nutrient intake. Lee *et al.* developed an intraoral sensor that measures sodium intake in real time for the management of hypertension.⁽¹⁴⁾ Among the nutrients contained in food and drink, glucose is directly linked to blood glucose levels and diabetes.⁽¹⁵⁾ In particular, glucose in drinks can easily cause blood glucose spikes owing to absorption from the small intestines.^(16,17) In this study, we designed a mouthguard (MG)-type sensor with an enzymatic glucose biosensor^(18,19) to quantify the glucose concentration of drinks in the oral cavity. The feasibility of the sensor was demonstrated through *in vitro* experiments using a dental phantom.

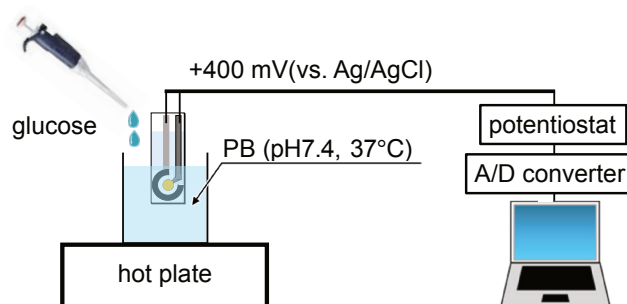
2 Materials and Methods

2.1 Evaluation for storability of glucose biosensor

Figure 1(a) shows the configuration of a glucose biosensor fabricated on MG material (polyethylene terephthalate glycol, ERKODENT Erich Kopp GmbH, Germany). The biosensor consisted of two electrodes: a Ag/AgCl reference/counter electrode and a Pt working electrode. The sensing area is the tip of the electrodes, which consists of an enzyme membrane layer



(a)



(b)

Fig. 1. (Color online) (a) Configuration of glucose biosensor. (b) Experimental setup for glucose measurement.

containing a mixture of glucose oxidase (GOD) and poly (MPC-co-EHMA-co-MBP) (PMEHB) and a PMEHB overcoating layer. The electrodes are covered with a polydimethylsiloxane (PDMS) insulator except for the sensing and terminal areas. In the sensing area, glucose is converted to gluconolactone (GDL) and hydrogen peroxide (H_2O_2) in an oxygenated environment in an enzyme-catalyzed reaction by GOD immobilized on the enzyme membrane layer. The produced H_2O_2 is oxidized at the Pt working electrode, and electrons are transferred with the Ag/AgCl counter electrode. The glucose concentration can be determined by measuring the output current with amperometry. The detailed fabrication process of the glucose biosensor followed that described in our previous study.⁽¹⁸⁾ The Pt working electrode was coated on the MG material using a parallel-plate sputtering machine (Canon Anelva Co.). The thickness and size of its sensing area were 200 nm and 1.6 mm², respectively. For the counter electrode, a Ag electrode was also coated with a thickness of 300 nm and a size of 16 mm² by sputtering. After coating the PDMS (Toray Dow Corning Co., Ltd.) insulator on the electrodes without the sensing and terminal areas, the Ag electrode was chloridized through electrochemical treatment in 0.1 mmol/L hydrochloric acid solution to form a Ag/AgCl electrode. To prepare the enzyme membrane layer, 2 μ L of PMEHB solution (5 wt% in ethanol), mixed with GOD (EC 1.1.3.4, 900 units/g, Sigma-Aldrich Co.) at a concentration of 15 units/ μ L, was applied to the Pt electrode in the sensing area. GOD was immobilized by crosslinking PMEHB with UV irradiation for 5 min. The PMEHB overcoating layer was also coated with PMEHB solution (1 wt% in ethanol).

The storability of the glucose biosensors was experimentally evaluated by comparing their output responses to a glucose solution with a certain concentration. The output current was measured every three days for the biosensors stored at +4 °C and those stored at -20 °C. The experimental setup for the output current measurement is shown in Fig. 1(b). The biosensor was immersed in phosphate buffer (PB), which was prepared at pH 7.4 and heated to 37 °C by a hot plate (REXIM RSH-1DN, AS ONE Corp., Japan). The terminal area of the biosensor was connected to a potentiostat (Model 1112, Husou electro chemical system, Japan). The potentiostat applied a constant voltage of +400 mV to the Pt electrode vs the Ag/AgCl electrode. A glucose solution was added to the PB at a concentration of 100 μ M, and the output current of the biosensor was measured by a PC via an A/D converter.

2.2 Measurement of glucose in soft drinks

The glucose concentration in some soft drinks was measured using the fabricated biosensor. First, with the same experimental setup shown in Fig. 1(b), a glucose solution was serially added to PB to reach a certain glucose concentration (1 μ M–20 mM), and the output current was measured to obtain reference calibration data. Afterward, an oral rehydration solution (OS-1, JAN: 4987035576419, Otsuka Pharmaceutical Factory, Inc., Japan) with a premeasured glucose concentration of 97.5 mM was also serially added to another PB to reach the same glucose concentration. Subsequently, the biosensor was immersed in the undiluted solution of OS-1, and a series of output current was also measured. The same experimental procedure was conducted using tap water instead of PB.

Glucose concentrations in commercially available coffee (JAN: 4901085199961, ITO EN, Ltd., Japan) and tea (JAN: 4909411091095, Kirin Holdings Co., Ltd., Japan) were also measured using the fabricated biosensor. The increase in output current was measured when 200 μL of each drink was added to 20 mL of tap water. The glucose concentration of each drink was calculated from the calibration equation obtained from the experimental results of adding OS-1 to tap water. The glucose concentration of each drink was measured using a commercially available glucose measurement kit (Glucose CII Test Wako, FUJIFILM Wako Pure Chemical Corp., Japan). Before measurement, 200 μL of each drink was mixed with 3 mL of coloring reagent and heated at 37 $^{\circ}\text{C}$ for 5 min. The absorbance at a wavelength of 505 nm of each drink was measured in a microplate reader (SH-1000Lab, Corona Electric Co., Ltd., Japan) and compared with that of a glucose standard solution.

2.3 Glucose measurement with a dental phantom

An MG-type glucose sensor was constructed by embedding the biosensor inside a double-layered MG. In this study, two types of prototype were fabricated: a wired prototype in which the biosensor was wired to an external potentiostat and a wireless prototype in which the Bluetooth Low Energy (BLE) potentiostat (customized, Discretek Inc., Japan) was sealed together inside the MG. First, the inner MG was formed on a dental phantom using a dental vacuum former (Vacuum adapter I, Yamahachi Dental MFG., Co., Japan), and the biosensor was attached to the side of the premolars and molars. In the case of the wireless prototype, a BLE potentiostat was also attached to the biosensor. Ag paste was used to wire the terminal area of the biosensor and the BLE potentiostat. Afterward, the separately prepared outer MG was overlaid on the inner MG, and both MGs were heat-welded using a heat gun. Finally, a through-hole was created in the outer MG to expose the sensing area of the biosensor. The BLE potentiostat and wireless prototype are shown in Fig. 2(a). The BLE potentiostat can transmit the output current of the biosensor to external devices via BLE communication. The dimensions of the BLE potentiostat are $12.3 \times 55 \times 4 \text{ mm}^3$, which make the potentiostat sufficiently small to be embedded in the MG.

Figure 2(b) shows the experimental setup for the *in vitro* evaluation of the MG-type glucose sensor. The MG-type glucose sensor was attached to the dental phantom, and two flow channels were prepared for the sensing area: one to deliver tap water and the other to deliver soft drinks. In the tap water channel, the prepared tap water was heated to 37 $^{\circ}\text{C}$ and pumped at a flow rate of 0.5 mL/min by a peristaltic pump (MP-1000, Tokyo Rikakikai Co., Ltd., Japan). In the soft drink channel, OS-1 was prediluted with tap water to glucose concentrations of 200, 500, and 1000 μM and pumped at a flow rate of 0.5 mL/min by another peristaltic pump (SJ-1211, ATTO Corp., Japan). At the beginning of the experiment, only the tap water channel was opened, and the output current of the sensor was allowed to stabilize. Thereafter, the active channel was switched from the tap water channel to the soft drink channel, and diluted OS-1 with a glucose concentration of 200 μM was introduced to the sensor. Subsequently, the channels were alternately switched to load diluted OS-1 with the glucose concentrations of 500 and 1000 μM in sequence. These experimental procedures were performed with both wired and wireless prototypes of the MG-type sensor.

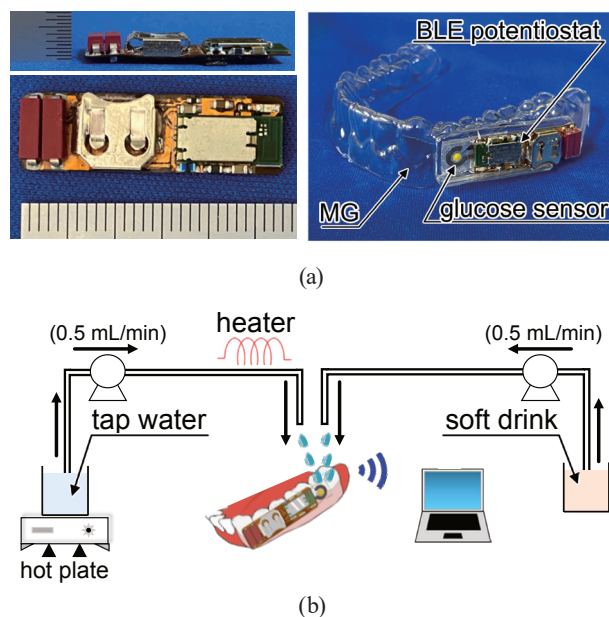


Fig. 2. (Color online) (a) Photo images of MG-type glucose biosensor with wireless data transmission capability. (b) Experimental setup for evaluation of MG-type glucose biosensor in a dental phantom.

3. Results and Discussion

3.1 Basic characteristics of the MG biosensor

Figures 3(a) and 3(b) show the output current responses of the biosensors stored at -20 and 4 $^{\circ}\text{C}$, respectively. The black, blue, and green lines in Figs. 3(a) and 3(b) represent the output responses to the solution with a glucose concentration of $100\ \mu\text{M}$ on the 1st, 27th, and 30th days after fabrication, respectively. Under both storage conditions, the output current increased with glucose loading up to the 30th day. The output current was $60\ \text{nA}$ on the 1st day; however, it decreased with the number of days. Figure 3(c) shows the trends in relative output based on the output current on the 1st day. Until about the 20th day after fabrication, the output was 90% or higher under both storage conditions. The output of the biosensors stored at -20 $^{\circ}\text{C}$ dropped significantly on the 24th day, and that of the biosensors stored at 4 $^{\circ}\text{C}$ also dropped on the 27th day. On the 30th day, the outputs of the biosensors under both storage conditions were 50% of that on the 1st day. These results demonstrated that the fabricated biosensor had high storability, showing the same output as the 1st day until the 27th day under the storage at 4 $^{\circ}\text{C}$.

3.2 Comparison of sensor outputs in different solutions

Figure 4(a) shows the output current responses of the biosensor when OS-1 was sequentially added to PB or tap water. Although there was a slight difference in initial output current between PB (black line) and tap water (red line), both results showed equivalent output characteristics for glucose loadings ranging from a few μM to a few mM . The output current of the biosensor

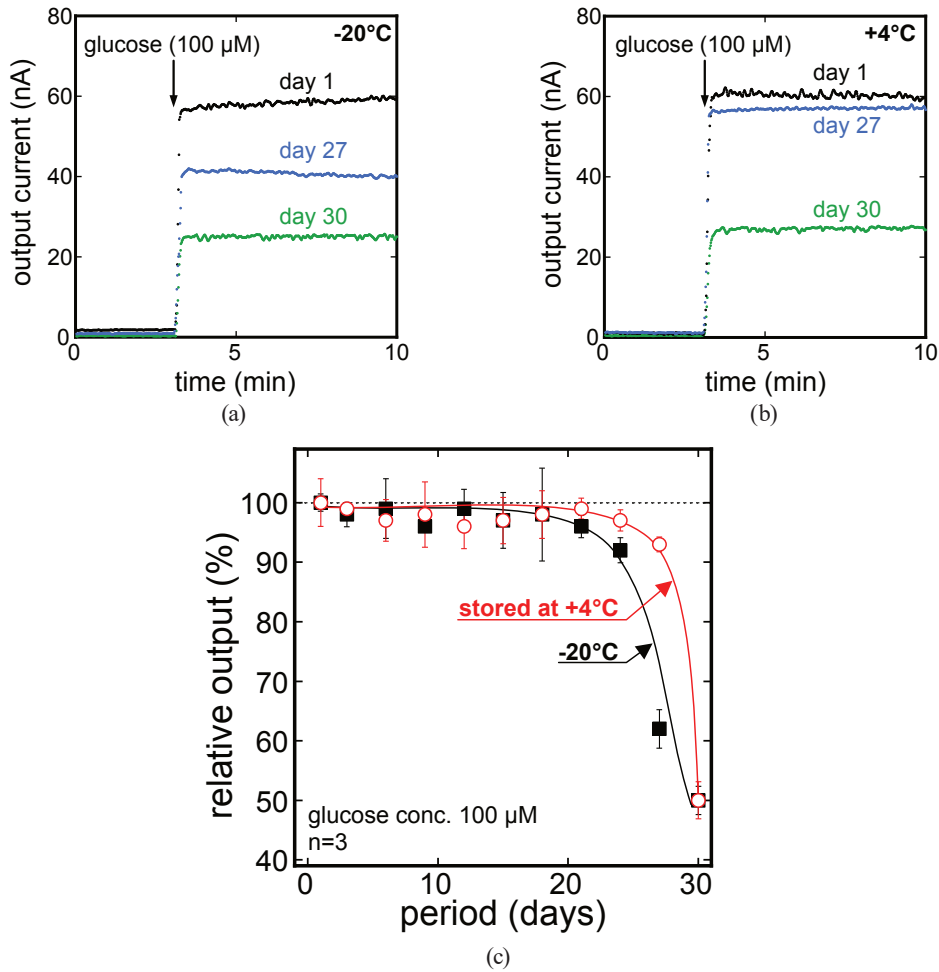


Fig. 3. (Color online) Response curves of biosensors stored at (a) -20 and (b) $+4$ °C on days 1, 27 and 30 after sensor fabrication. (c) Effect of storage temperature on storability of biosensors. Open circles and filled squares indicate storage temperatures of $+4$ and -20 °C, respectively.

saturated at glucose concentrations above 10 mM, including the undiluted OS-1. The output currents for each glucose concentration are summarized in Fig. 4(b). This figure also shows the experimental results obtained when a glucose solution was added to PB. These three experimental results showed an equivalent relationship between glucose concentration and output current. The calibration equations identified from these results are shown as follows:

$$\text{Current (nA)} = 0.34398 \times [\text{glucose } (\mu\text{M})]^{1.0453}, \quad (1)$$

$$\text{Current (nA)} = 0.35579 \times [\text{glucose } (\mu\text{M})]^{0.96935}, \quad (2)$$

$$\text{Current (nA)} = 0.62744 \times [\text{glucose } (\mu\text{M})]^{1.0239}. \quad (3)$$

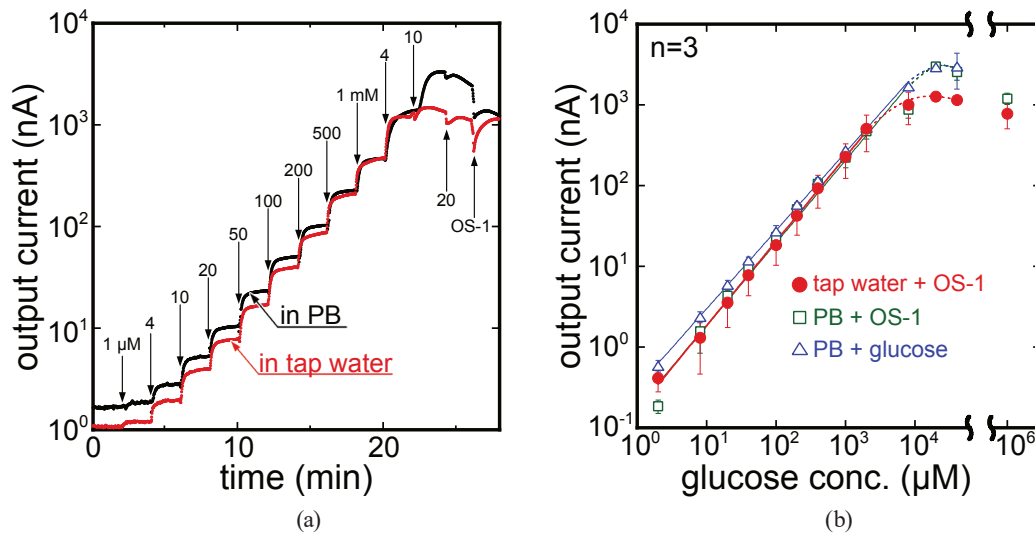


Fig. 4. (Color online) (a) Responses of glucose biosensor against various concentrations of glucose in OS-1 at PB or tap water. (b) Comparison of calibration curves under different measurement conditions. Filled circles, open squares, and open triangles indicate tap water + OS-1, PB + OS-1, and PB + pure glucose, respectively.

Equation (1) represents the calibration equation for tap water and OS-1. The quantification range was 1 μM –1 mM, and the coefficient of determination, R , was 0.9988. Equation (2) represents the calibration equation for PB and OS-1. The quantification range was 1 μM –4 mM with $R = 0.9973$. Equation (3) represents the calibration equation for PB and glucose solution. The quantification range was 1 μM –4 mM with $R = 0.9143$. Both calibration equations showed equivalent characteristics, suggesting that tap water can be used as a potable solvent or diluent instead of PB.

3.3 Evaluation of quantification accuracy for glucose in different soft drinks

Figure 5 shows the results of glucose concentration measurements for coffee, tea, and OS-1. The white bars represent the measurement results obtained using the glucose measurement kit, and the shaded bars represent the measurement results obtained using the biosensor. For the biosensor, the glucose concentration of each soft drink was calculated by substituting the output current into Eq. (3). The measurement results for coffee, tea, and OS-1 were 2.5, 2.1, and 104.8 mM, respectively. On the other hand, the glucose measurement kit indicated that the glucose concentrations of the soft drinks were 4.2, 4.0, and 97.5 mM, respectively. Because the glucose measurement kit utilized an absorbance measurement, it is possible that the measurement results for the coffee and tea were higher than the actual values. However, the measurement results obtained using the biosensor and the glucose measurement kit showed the same trend, indicating that the fabricated biosensor can measure the glucose concentration of each soft drink after dilution to a concentration within the quantification range.

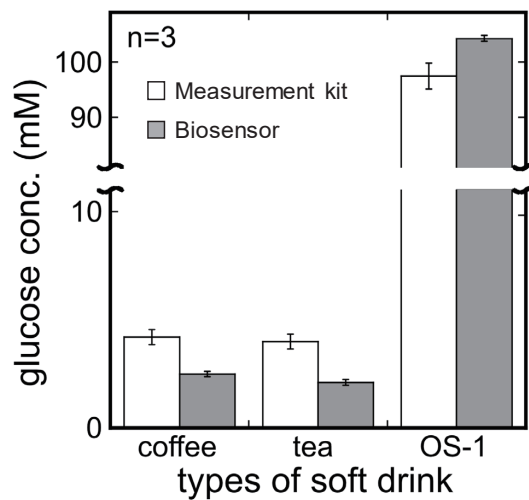


Fig. 5. Comparison of glucose concentration measurements obtained using standard method and glucose biosensor for coffee, tea, and OS-1.

3.4 Demonstration of glucose monitoring with a dental phantom

Figure 6(a) shows the output current response of the wired prototype of the MG-type sensor when loaded with diluted OS-1. The output current increased clearly in response to the loading of diluted OS-1 at each glucose concentration. Figure 6(b) shows a comparison of the output current of the wired MG type with that of the sheet type, which is the biosensor without embedding in MG as already shown in Fig. 4(b). The output currents of the wired MG-type sensor for OS-1 diluted to glucose concentrations of 200, 500, and 1000 μM were in good agreement with the calibration results of the sheet type. These results indicate that the wired MG-type sensor can quantify glucose concentration as well as the sheet-type sensor without the effect of embedding in the MG.

Figure 6(c) shows the output current response of the wireless prototype of the MG-type sensor when loaded with diluted OS-1. As with the wired prototype, the output current of the wireless prototype increased clearly in response to the diluted OS-1 with the glucose concentrations of 200, 500, and 1000 μM . However, the magnitude of the output current for each concentration was lower than that of the wired prototype. The output currents of the wired and wireless prototypes for each glucose concentration are summarized in Fig. 6(d). Although the output currents of the wireless prototype for each glucose concentration were one-fifth to one-sixth that of the wired prototype, the output variation with glucose concentration was consistent in both prototypes, indicating the possibility of quantifying glucose concentration using the wireless MG-type sensor with appropriate calibration.

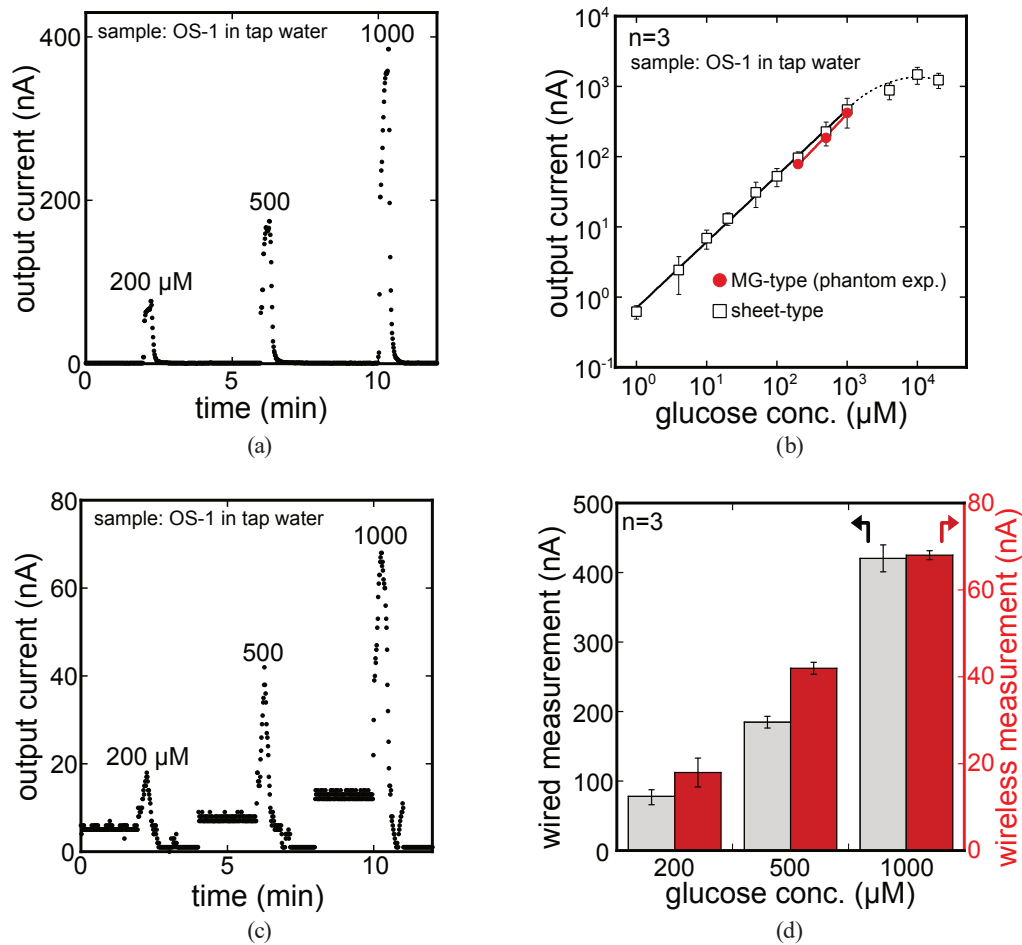


Fig. 6. (Color online) (a) Response of MG-type biosensor against glucose with wired measurement setup. (b) Comparison of the standard calibration curve and concentration dependence in a dental phantom experiment. (c) Response of MG-type biosensor against glucose with wireless measurement setup. (d) Comparison of wired and wireless measurement results.

4. Conclusions

In this study, we proposed an MG-type sensor for the real-time measurement of the glucose concentration of ingested drinks with an enzymatic biosensor. The GOD-immobilized sheet-type biosensor was fabricated, which showed high storability maintaining output characteristics for up to 27 days under +4 $^{\circ}\text{C}$. We demonstrated that the sheet-type sensor could quantify the glucose concentrations of drinks such as coffee and tea equivalent to commercial glucose measurement kits. An MG-type sensor integrating the sheet-type biosensor was also fabricated. This MG-type sensor showed the output equivalent to the bare biosensor in the wired measurement, and the wireless measurement using a BLE potentiostat also showed proportional output. These experimental results indicate a potential application of real-time drink glucose concentration measurement in the oral cavity for the management and prevention of diabetes.

Acknowledgments

This work was supported by the Japan Society for the Promotion of Science (JSPS) KAKENHI Grant Numbers JP24K00893 and JP19KK0259, and the Cooperative Research Project of the Research Center for Biomedical Engineering.

References

- 1 A. Berbudi, N. Rahmadika, A. I. Tjahjadi, and R. Ruslami: *Current Diabetes Reviews* **16** (2020) 442. <https://doi.org/10.2174/1573399815666191024085838>
- 2 S. H. Ley, O. Hamdy, V. Mohan, and F. B. Hu: *The Lancet* **383** (2014) 1999. [https://doi.org/10.1016/S0140-6736\(14\)60613-9](https://doi.org/10.1016/S0140-6736(14)60613-9)
- 3 L. Johnston, G. Wang, K. Hu, C. Qian, and G. Liu: *Front. Bioeng. Biotechnol.* **9** (2021) 733810. <https://doi.org/10.3389/fbioe.2021.733810>
- 4 Z. Pu, X. Zhang, H. Yu, J. Tu, H. Chen, Y. Liu, X. Su, R. Wang, L. Zhang, and D. Li: *Sci. Adv.* **7** (2021) eabd0199. <https://doi.org/10.1126/sciadv.abd0199>
- 5 V. P. Rachim and W.-Y. Chung: *Sens. Actuators, B* **286** (2019) 173. <https://doi.org/10.1016/j.snb.2019.01.121>
- 6 Y. Guo, Z. Huang, D. Sang, Q. Gao, and Q. Li: *Front. Bioeng. Biotechnol.* **8** (2020) 575442. <https://doi.org/10.3389/fbioe.2020.575442>
- 7 N. A. Kong, F. M. Moy, S. H. Ong, G. A. Tahir, and C. K. Loo: *Digital Health* **9** (2023) 20552076221149320. <https://doi.org/10.1177/20552076221149320>
- 8 A. Myers, N. Johnston, V. Rathod, A. Korattikara, A. Gorban, N. Silberman, S. Guadarrama, G. Papandreou, J. Huang, and K. Murphy: 2015 IEEE Int. Conf. Computer Vision (ICCV) (IEEE, 2015) 1233–1241.
- 9 Z. Shen, A. Shehzad, S. Chen, H. Sun, and J. Liu: *Procedia Comput. Sci.* **174** (2020) 448. <https://doi.org/10.1016/j.procs.2020.06.113>
- 10 N. A. Selamat and S. H. Md. Ali: *IEEE Access* **8** (2020) 48846. <https://doi.org/10.1109/ACCESS.2020.2978260>
- 11 H. L. McClung, L. T. Ptomey, R. P. Shook, A. Aggarwal, A. M. Gorczyca, E. S. Sazonov, K. Becofsky, R. Weiss, and S. K. Das: *American Journal of Preventive Medicine* **55** (2018) e93. <https://doi.org/10.1016/j.amepre.2018.06.011>
- 12 K. Iitani, K. Kishima, Y. Kasuga, K. Yokota, H. Nitta, K. Onchi, G. Kawase, K. Umezawa, K. Toma, T. Arakawa, D. V. Dao, and K. Mitsubayashi: *Sens. Mater.* **35** (2023) 1315. <https://doi.org/10.18494/SAM4218>
- 13 K. Ichikawa, K. Iitani, G. Kawase, K. Toma, T. Arakawa, D. V. Dao, and K. Mitsubayashi: *Sensors* **24** (2024) 1436. <https://doi.org/10.3390/s24051436>
- 14 Y. Lee, C. Howe, S. Mishra, D. S. Lee, M. Mahmood, M. Piper, Y. Kim, K. Tieu, H.-S. Byun, J. P. Coffey, M. Shayan, Y. Chun, R. M. Costanzo, and W.-H. Yeo: *PNAS* **115** (2018) 5377. <https://doi.org/10.1073/pnas.1719573115>
- 15 L. Bonsembiante, G. Targher, and C. Maffei: *Nutrients* **13** (2021) 3344. <https://doi.org/10.3390/nu13103344>
- 16 L. V. Gromova, S. O. Fetissov, and A. A. Gruzdkov: *Nutrients* **13** (2021) 2474. <https://doi.org/10.3390/nu13072474>
- 17 V. S. Malik, B. M. Popkin, G. A. Bray, J.-P. Després, and F. B. Hu: *Circulation* **121** (2010) 1356. <https://doi.org/10.1161/CIRCULATIONAHA.109.876185>
- 18 T. Arakawa, K. Tomoto, H. Nitta, K. Toma, S. Takeuchi, T. Sekita, S. Minakuchi, and K. Mitsubayashi: *Anal. Chem.* **92** (2020) 12201. <https://doi.org/10.1021/acs.analchem.0c01201>
- 19 A. Wiorek, M. Parrilla, M. Cuartero, and G. A. Crespo: *Anal. Chem.* **92** (2020) 10153. <https://doi.org/10.1021/acs.analchem.0c02211>